

VIP Enhances Phagocytosis of Fibrillar Beta-Amyloid by Microglia and Attenuates Amyloid Deposition in the Brain of APP/PS1 Mice

Min Song^{1,3}, Jia-xiang Xiong^{2,3}, Yan-yan Wang¹, Jun Tang¹, Bo Zhang¹, Yun Bai^{1*}

1 Department of Medical Genetics, Third Military Medical University, ChongQing, China, **2** Department of Medical Physiology, Third Military Medical University, ChongQing, China

Abstract

Vasoactive intestinal peptide (VIP) is a multifunctional neuropeptide with demonstrated immunosuppressive and neuroprotective activities. It has been shown to inhibit Amyloid beta (A β)-induced neurodegeneration by indirectly suppressing the production and release of a variety of inflammatory and neurotoxic factors by activated microglia. We demonstrated that VIP markedly increased microglial phagocytosis of fibrillar A β 42 and that this enhanced phagocytotic activity depended on activation of the Protein kinase C (PKC) signaling pathway. In addition, VIP suppressed the release of tumor necrosis factor alpha (TNF- α) and nitric oxide (NO) from microglia activated by combined treatment with fibrillar A β 42 and low dose interferon- γ (IFN- γ). We utilized an adenovirus-mediated gene delivery method to overexpress VIP constitutively in the hippocampus of APPswPS1 transgenic mice. The A β load was significantly reduced in the hippocampus of this animal model of Alzheimer's disease, possibly due to the accumulation and activation of cd11b-immunoreactive microglial cells. The modulation of microglial activation, phagocytosis, and secretion by VIP is a promising therapeutic option for the treatment of Alzheimer's disease (AD).

Citation: Song M, Xiong J-x, Wang Y-y, Tang J, Zhang B, et al. (2012) VIP Enhances Phagocytosis of Fibrillar Beta-Amyloid by Microglia and Attenuates Amyloid Deposition in the Brain of APP/PS1 Mice. PLoS ONE 7(2): e29790. doi:10.1371/journal.pone.0029790

Editor: Michelle L. Block, Virginia Commonwealth University, United States of America

Received: May 19, 2011; **Accepted:** December 5, 2011; **Published:** February 6, 2012

Copyright: © 2012 Song et al. This is an open-access article distributed under the terms of the Creative Commons Attribution License, which permits unrestricted use, distribution, and reproduction in any medium, provided the original author and source are credited.

Funding: This work was supported by National Natural Science Foundation of China (NO. 81000147, NO.30228018) and the funders had no role in study design, data collection and analysis, decision to publish, or preparation of the manuscript.

Competing Interests: The authors have declared that no competing interests exist.

* E-mail: baiyungene@gmail.com

³ These authors contributed equally to this work.

Introduction

Alzheimer's disease is a progressive neurodegenerative disease characterized by senile plaques, intracellular neurofibrillary tangles, and reactive gliosis involving both microglia and astrocytes [1,2]. Microglia are derived from mononuclear phagocytes and function as the resident macrophage-like cells of the brain parenchyma. Microglia serve functions similar to other resident macrophages, including phagocytosis, antigen presentation and production of cytokines. Microglia-mediated immune responses play both protective and deleterious roles in the pathogenesis of AD. On one hand, microglia secrete neurotrophic agents and eliminating beta-amyloid through direct phagocytosis. Conversely, microglia release neurotoxic (pro-inflammatory) cytokines and other factors that can cause neurodegeneration, including NO. Therapeutic strategies that inhibit the secretion of neurotoxins from microglia or enhance microglial phagocytic activity may reduce cerebral A β load in mouse models of AD and thus limit neurodegeneration [3–6].

Several endogenous brain mechanisms serve to dampen inflammatory responses in the brain. As one group of critical anti-inflammatory agents, neuropeptides maintain the immunological privilege of the central nerve system (CNS) [7]. For example, calcitonin gene-related peptide [8], adrenomedullin [9], neuropeptide Y [10] and somatostatin [11] are anti-inflammatory immune modulators. Several recent studies indicated that

vasoactive intestinal peptide can also modulate immune function through G-protein coupled receptors expressed by immune cells and that VIP signaling is an important component of a homeostatic neuroimmune control system [12][13]. Vasoactive intestinal peptide is a 28-amino acid peptide secreted by peptidergic neurons located in all regions of the cerebral cortex, limbic forebrain (septum, amygdala, hippocampus, and stria terminalis) and hypothalamic areas (paraventricular and periventricular nuclei, arcuate nucleus, and anterior and preoptic areas). It is believed that VIP-containing nerve terminals constitute an anatomical link between the CNS and immune system [14–16].

Vasoactive intestinal peptide exerts anti-inflammatory effects on microglia by activating two common VIP receptors: VPAC1 and VPAC2. These receptors stimulate adenylate cyclase (AC), which increases intracellular cyclic adenosine monophosphate (cAMP) concentrations and leads to downstream activation of protein kinase A (PKA) and PKA-responsive transcription factors. The release of pro-inflammatory TNF- α , interleukin(IL)-1 β , IL-6, NO from bacterial lipopolysaccharide (LPS)-activated primary microglial cultures was markedly reduced by 10⁻⁸ M VIP [17][18]. Lipopolysaccharide and interferon gamma (IFN- γ)-activated microglia also produced less macrophage inflammatory protein (MIP)-2, MIP-1 α , keratinocyte derived chemokine (KC), RANTES (regulated upon activation normal T cell expressed and secreted protein and γ -interferon inducible protein (IP-10) in response to VIP treatment [17] [19]. Thus, VIP stimulation of

activated microglia reduces the secretion of a multitude of proinflammatory chemokines and cytokines. Expression of VIP is significantly decreased in the cerebral cortex of aged animals and VIP blockade in younger animals resulted in impaired learning and memory [20–21].

In addition, VIP secretion was significantly reduced in the insular and angular cortex of AD patients as measured by radioimmunoassay [22], while the number of neurons expressing VIP was significantly reduced in the suprachiasmatic nucleus of female pre-senile AD patients [23]. It is still unclear, however, whether this reduction was the cause or the result of cortical deterioration and AD-related cognitive decline. A recent study did manage to show that VIP inhibited A β -induced neurodegeneration by indirectly inhibiting the production of a battery of inflammatory and neurotoxic agents by activated microglia cells [24], suggesting that a VIP deficit may contribute to AD-associated focal cortical degeneration. Whether VIP treatment to the brain can improve AD pathogenesis has still not been demonstrated. Furthermore, increased phagocytic capacity of microglia after VIP treatment, a possible mechanism to reduce cerebral A β load, has also not been directly observed.

The present study investigated the effect of VIP on the phagocytosis of A β by microglia and on the secretion of proinflammatory cytokines by microglia in response to A β . To demonstrate the beneficial effect of VIP *in vivo*, we overexpressed VIP in transgenic PS1/APP mice and examined whether this treatment could decrease brain A β load in this AD model.

Results

VIP promote phagocytosis of fibrilized A β_{1-42} by activated murine microglial cells

We first examined the effects of VIP on the phagocytic functions of mouse primary microglial cells. To determine if VIP can modulate microglial uptake of A β_{1-42} , mouse primary microglial cells were incubated in 500 nM fibrilized-Cy3-A β_{1-42} for 2 h in the presence or absence of VIP. Cell supernatants and lysates were analyzed for extracellular and cell-associated Cy3-A β_{42} using a fluorometer (Fig. 1A, B). Co-incubation with VIP significantly enhanced microglial phagocytosis of A β_{1-42} peptide as evidenced by the increase in cell-associated Cy3-A β_{42} fluorescence (Fig. 1A, top panel) and the significant reduction in extracellular Cy3-A β_{42} (Fig. 1A, bottom panel). As a control for the non-phagocytic incorporation of A β_{1-42} by microglia, microglial cells were incubated at 4°C under the same treatment conditions. As a positive control, Cy3-A β_{42} uptake was measured in the presence of the ubiquitous microglial activator LPS; indeed LPS increased microglial phagocytic Cy3-A β_{42} uptake (Fig. 1A, top panel) and reduced extracellular Cy3-A β_{42} (Fig. 1A, bottom panel, $P < 0.05$). We next assessed the effect of different VIP doses on microglial phagocytosis of fibrilized-A β_{1-42} . Phagocytotic uptake was dependent on VIP dose, with maximal intracellular Cy3-A β_{42} at 10^{-6} M (Fig. 1B, $P < 0.05$). This enhanced A β_{42} phagocytosis was verified by a quantitative immunofluorescence assay. Cultures were incubated in fluorescence-tagged A β_{42} in the presence and absence of VIP. Cultured microglia exhibited significantly higher intracellular fluorescence when cultured in the presence of VIP (Fig. 1C).

PKC inhibitors attenuate VIP-enhanced phagocytosis of fibrilized-A β_{42} by microglia

Delgado et al. found that the stimulatory effect of VIP on freshly isolated resting macrophages was mediated by the PKC signaling pathway [25]. To examine the signal pathways involved in VIP-

mediated stimulation of microglial phagocytosis of fibrilized-A β_{42} , microglial cultures were treated with VIP for 2 hr in the presence of the myristoylated protein kinase C peptide inhibitor or the PKA inhibitor fragment 14–22, myristoylated trifluoroacetate salt. In parallel experiments, microglial cultures were treated with the PKC agonist PMA or the adenylyl cyclase/PKA pathway activator forskolin. Forskolin treatment alone did not enhance Cy3-A β_{42} phagocytosis compared to controls. In contrast, PKC activation by PMA increase microglia phagocytic activity compared to controls. The PKC pathway inhibitor myristoylated protein kinase C peptide inhibitor abolished the increased phagocytosis of Cy3-A β_{42} induced by VIP, while the PKA inhibitor fragment 14–22 had no effect (Fig. 2 A,B). These data suggest that activation of the PKC pathway, but not the PKA pathway, is necessary for the VIP-induced enhancement of Cy3-A β_{42} phagocytosis by microglial cells.

VIP inhibits A β_{42} -activated TNF- α and NO secretion from murine microglial cells

Activated microglia can be either neuroprotective or neurodestructive depending on the phase of activation. VIP may promote neuroprotection against A β toxicity by promoting phagocytosis. To examine whether VIP also altered the secretion of neurotoxic cytokines or oxidant species, the levels of TNF- α and NO were measured in the supernatant of activated microglia in the presence and absence of VIP. Murine primary microglial cells were activated with either fibrilized A β_{1-42} (2.5 μ M) alone or fibrilized A β_{1-42} combined with low dose IFN- γ (10 U/ml) for 24 h in the absence or presence of VIP. The secretion of TNF- α and NO were analyzed by ELISA. Low dose IFN- γ plus A β_{1-42} evoked a robust increase in TNF- α and NO secretion [26]. Treatment with VIP alone (10^{-8} M) did not affect basal TNF- α and NO secretion from resting microglia (Fig. 3A,B) but inhibited TNF- α and NO secretion induced by A β plus low dose IFN- γ (Fig. 3A,B, $P < 0.01$). Similar results were obtained in the murine microglial cell line N9 cells (data not shown). Thus, VIP could enhance phagocytosis of A β_{42} by activated microglia and inhibit the release of neurotoxic TNF- α and NO by A β_{42} -activated microglia.

Adenovirus-mediated VIP expression reduces immunoreactive A β deposits and fibrillar A β deposits in the hippocampus but not in the neocortex of AD mice

We next determined whether VIP treatment could affect A β plaque formation and accumulation in a mouse model of Alzheimer's disease. Since exogenous VIP is rapidly degraded [27], we adopted viral vectors for sustained and local expression of a VIP transgene. We constructed a recombinant adenovirus vector encoding functional VIP, Ad-VIP (Fig. 4A), as described previously [28]. The infectious titer of the Ad-VIP vector was 1.0×10^{11} pfu/mL. Expression of VIP protein was determined in virus-infected 293 cells. Typically, 2×10^2 particles of Ad-VIP vector/cell resulted in an almost 20-fold increase of VIP in the culture medium per 10^6 infected 293 cells (Fig. 4C).

We then stereotaxically injected the recombinant fluorescence-labeled adenovirus Ad-VIP into the right lateral ventricle of 10 month old PS1/APPsw mice (expressing mutant APP and PS1). A control group of PS1/APPsw mice were injected with a blank recombinant adenovirus, Ad-Blank, or with PBS. After two months, mice were sacrificed and VIP expression was quantified by red fluorescence distribution and intensity. Widespread and intense fluorescence was observed in the dentate gyrus (DG). Combined staining of neuronal cell bodies with NeuN revealed that Ad-VIP could be efficiently expressed in DG granule and hilar neurons for as long as two months (Fig. 4D).

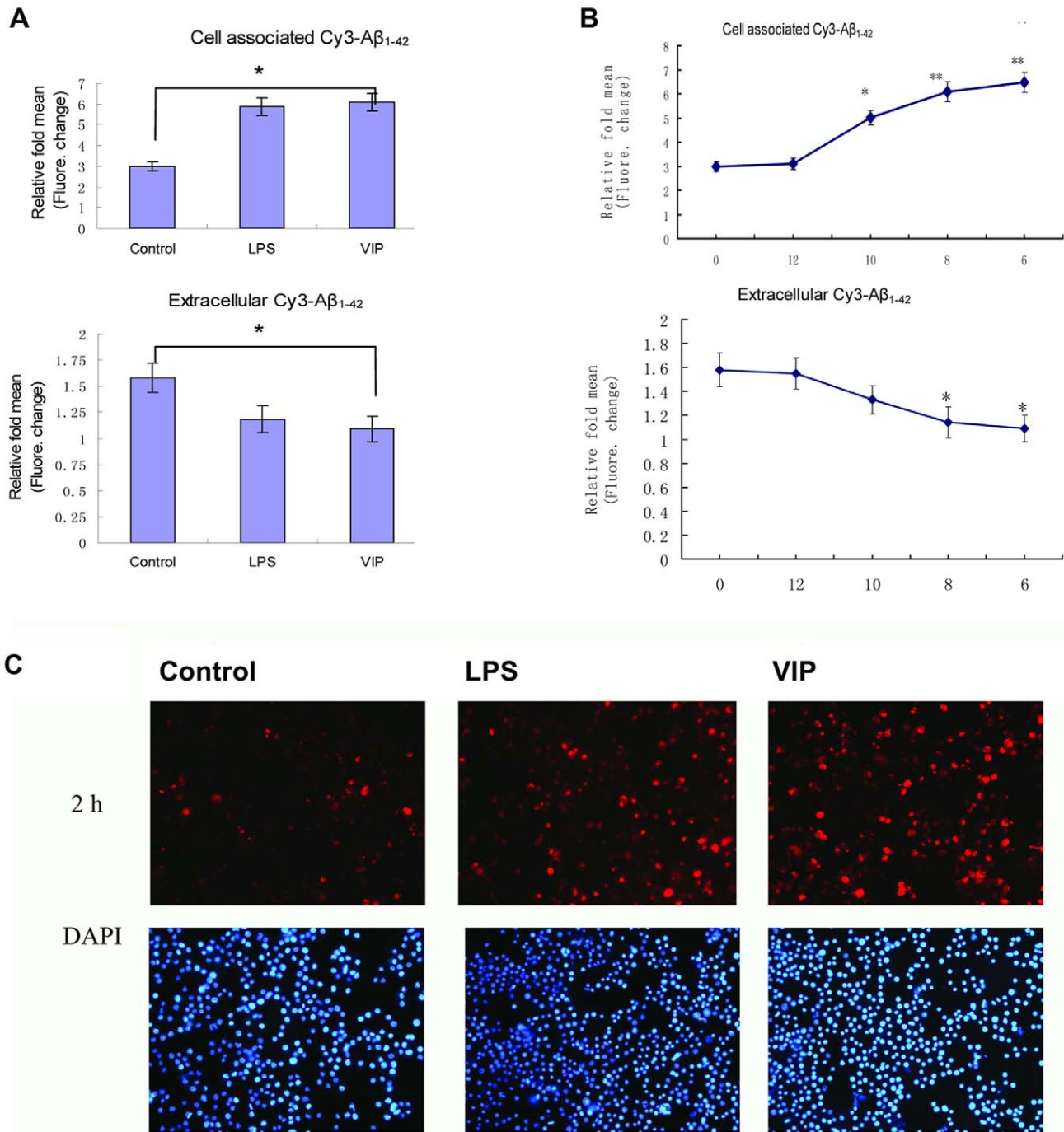


Figure 1. VIP treatment promote microglial phagocytosis of fibrillar A β_{1-42} . A: Cell supernatants and lysates were analyzed for cell-associated (top panel) and extracellular (bottom panel) Cy3-A β_{1-42} using a fluorometer. Data are represented as the relative fold of mean fluorescence change (mean \pm SD), calculated as the mean fluorescence for each sample at 37°C divided by mean fluorescence at 4°C (n=5 for each condition presented). One-way ANOVA followed by post-hoc comparison showed a significant between-group difference (*P<0.05, **P<0.01 compared with control). B: Primary microglia cells were stimulated with fibrillar A β_{1-42} (500 nM) in the absence or presence of different concentrations of VIP (-logM). Cell supernatants and lysates were analyzed for cell-associated (right panel) and extracellular (left panel) Cy3-A β_{1-42} using a fluorometer (n=5 for each condition presented). C: Mouse primary microglial cells were seeded in twelve-well tissue-culture plates (2×10^5 /well) and treated with 500 nM Cy3-A β_{1-42} in the presence or absence of VIP (10^{-8} M), LPS (100 ng/ml, as positive control). After 2 hr, these cells were washed and fixed (see Materials and Methods). Subsequently, immunofluorescence microscopy examination was performed with a $\times 10$ objective with appropriate filter selection. The up panels show Cy3-A β_{1-42} associated with microglial cells under the various treatment conditions. The below panels (DAPI) reveal the presence of the microglia cell as identified by their nuclei.
doi:10.1371/journal.pone.0029790.g001

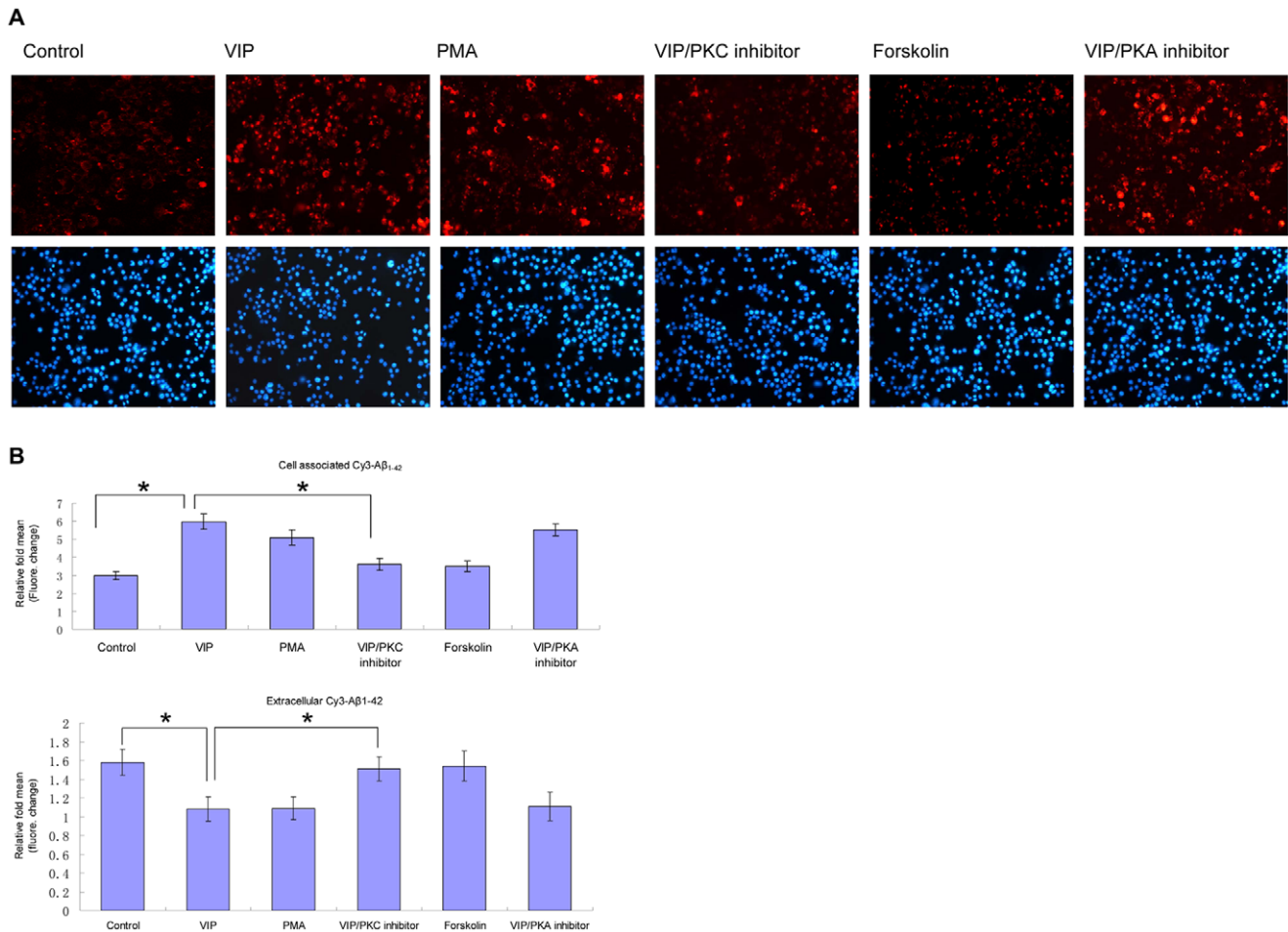


Figure 2. PKC inhibitor attenuates VIP promotion of microglial phagocytosis of fibrillar A β ₁₋₄₂. A: Mouse primary microglial cells were seeded in twelve-well tissue-culture plates (2×10^5 /well) and treated with 500 nM Cy3-A β ₁₋₄₂ in the presence of VIP (10^{-8} M), PMA (30 nM), Forskolin (10 μ M), Myristoylated protein kinase C peptide (50 μ M) combined with VIP, PKA inhibitor fragment 14–22 myristoylated trifluoroacetate salt (PKA Inhibitor) (5 μ M) combined with VIP. After 2 hr, these cells were washed and fixed (see Materials and Methods). Subsequently, immunofluorescence microscopy examination was performed with a $\times 10$ objective with appropriate filter selection. The up panels show Cy3-A β ₁₋₄₂ associated with microglial cells under the various treatment conditions. The below panels (DAPI) reveal the presence of the microglia cell as identified by their nuclei. B: Mouse primary microglial cells were seeded in twelve-wells tissue-culture plates (2×10^5 /well) and treated with 500 nM Cy3-A β ₁₋₄₂ in the presence or absence of VIP and Myristoylated protein kinase C peptide inhibitor, PMA (PKC pathway activator), cAMP agonists (Forskolin), PKA antagonists (PKA inhibitor fragment 14–22, myristoylated trifluoroacetate salt) for 2 hr. Subsequently, Cell supernatants and lysates were analyzed for cell-associated (top panel) and extracellular (bottom panel) Cy3-A β ₁₋₄₂ using a fluorometer. Data are represented as the relative fold of mean fluorescence change (mean \pm SD), calculated as the mean fluorescence for each sample at 37°C divided by mean fluorescence at 4°C (n = 5 for each condition presented). One-way ANOVA followed by post-hoc comparison showed a significant between-group difference (* $P < 0.05$, ** $P < 0.01$ compared with control). doi:10.1371/journal.pone.0029790.g002

To determine the efficacy of adenovirus-mediated VIP expression in reducing A β load in the brain, diffuse and fibrillar A β deposits were detected by immunohistochemistry using the anti-A β 6E10 antibody and quantified by morphometry (Fig. 5A, a–c and 5B). The amyloid load was expressed as the percent area showing A β immunoreactivity. The average A β load in hippocampus was $0.39 \pm 0.09\%$ in the Ad-VIP-injected group, significantly lower than in either the Ad-Blank group ($0.65 \pm 0.15\%$) or the PBS-injected group ($0.70 \pm 0.06\%$) (Fig. 6B). Thus, Ad-VIP injection reduced the A β load in the hippocampus by approximately 40% compared to the blank vector ($P = 0.04$, n = 8 for each group). In the neocortex, however, the average amyloid load in Ad-VIP-injected mice ($1.25 \pm 0.10\%$) not significantly less than in Ad-blank-injected mice ($1.34 \pm 0.17\%$) or PBS-injected mice ($1.32 \pm 0.15\%$) (Ad-VIP vs. PBS, $P = 0.66$).

Fibrillar A β deposits were detected by thioflavin S staining and quantified by morphometric analysis (Fig. 5A, d–f and 5C). Again,

the A β loads were quantified by the average percent area showing thioflavin S fluorescence. The average hippocampal A β load in Ad-VIP-injected mice ($0.39 \pm 0.03\%$) was significantly lower than in Ad-blank-injected mice ($0.53 \pm 0.03\%$) and PBS-injected mice ($0.57 \pm 0.04\%$). Thus, Ad-VIP injection reduced thioflavin S staining in the hippocampus by approximately 25% compared to Ad-blank injection ($P = 0.01$, n = 8 for each group). In the neocortex, there was no difference in the A β load as measured by thioflavin S fluorescence between any of the mouse treatment groups (Fig. 5C).

We further determined the levels of buffer-soluble and insoluble A β in the treatment groups by A β ₄₀- and A β ₄₂-specific sandwich ELISAs. In the hippocampus, the buffer-soluble A β ₄₂ content in Ad-VIP-injected mice (45.97 ± 2.57 pg/mg protein) was significantly lower than in Ad-blank-injected mice (61.65 ± 4.5 pg/mg protein) and PBS-injected mice (57.29 ± 6.48 pg/mg protein) (Figure 6A). Injection of Ad-VIP reduced the buffer-soluble A β ₄₂ level in the hippocampus by approximately 27% compared to Ad-

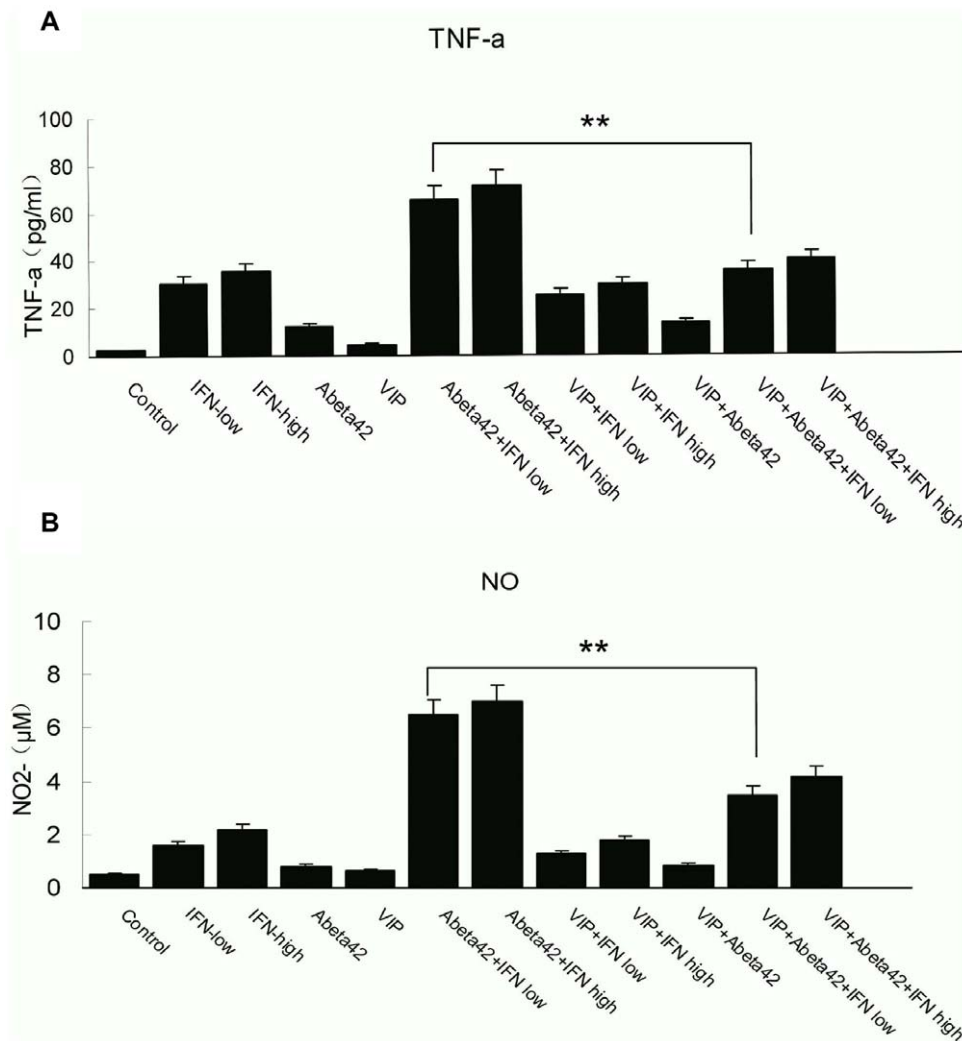


Figure 3. VIP inhibit TNF- α or NO secretion induced by A β_{1-42} (2.5 μ M) combined with low dose IFN- γ (10 U/ml) in microglial cells. Microglial cells were plated in 24-well tissue-culture plates at 1×10^5 cells per well and stimulated for 24 hr with either A β_{1-42} (2.5 μ M) or a dose range of 10 U/mL IFN- γ (IFN low), 200 U/mL IFN- γ (IFN high)/A β_{1-42} (2.5 μ M) in the presence or absence of VIP (10^{-8} M). Cell-free supernatants were collected and subjected to TNF- α ELISA or Nitrite Determination Griess Reagent Kit as indicated. Data are the mean \pm SD of three separate experiments performed in double duplicate. ANOVA and post hoc testing revealed significant differences between different group. ****** $P < 0.01$ A β_{1-42} /IFN- γ treated samples plus VIP vs. A β_{1-42} /IFN- γ treated samples. doi:10.1371/journal.pone.0029790.g003

blank injection ($P = 0.011$, $n = 7$ for each group). The buffer-soluble A β_{40} content in Ad-VIP-injected transgenic mice (44.04 ± 3.98 pg/mg protein, $n = 7$) was also significantly lower than in Ad-Blank-injected mice (66.90 ± 7.86 pg/mg protein, $n = 7$, $P = 0.03$) (Fig. 6B). The buffer-insoluble A β_{42} and A β_{40} in Ad-VIP-injected mice (74.82 ± 5.88 ng/mg protein and 61.15 ± 5.36 ng/mg protein, respectively) was moderately reduced compared to the Ad-blank-injected mice (89.32 ± 5.04 ng/mg protein, 76.50 ± 8.27 ng/mg protein, respectively) and PBS-injected mice (85.19 ± 5.31 ng/mg protein, 74.24 ± 2.92 ng/mg protein, respectively), but the difference did not reach statistical significance (Ad-VIP vs. Ad-Blank, $P = 0.13$ for insoluble A β_{42} , $P = 0.12$ for insoluble A β_{40}) (Fig. 6C, D).

In the neocortex, buffer-soluble A β_{42} in Ad-VIP-injected mice (45.71 ± 5.41 pg/mg protein) was not significantly lower than in Ad-blank-injected mice (48.18 ± 6.91 pg/mg protein) or PBS-injected mice (50.94 ± 4.43 pg/mg protein) (Ad-VIP vs. PBS, $P = 0.47$). There was no difference in the insoluble A β_{42} or insoluble A β_{40} between any treatment groups (Fig. 6C).

Ad-VIP injection activated CD11b-immunoreactive microglial in the hippocampus, but not CD11c- or CD45-immunoreactive microglia

The role of microglial activation in A β plaque reduction in PS1/APP^{sw} mice was investigated by immunofluorescence labeling (Fig. 7). The average CD11b immunoreactive area in the hippocampus was $0.21 \pm 0.03\%$ in Ad-VIP-injected mice, $0.14 \pm 0.03\%$ in Ad-Blank-injected mice, and $0.11 \pm 0.03\%$ in mice injected with PBS (Fig. 7A, a-c, 7B). Thus, Ad-VIP injection enhanced the accumulation of CD11b-immunoreactive microglial cells in the hippocampus by approximately 50% compared to Ad-Blank injection ($P = 0.003$, $n = 8$ for each group). However, the numbers of CD11c-immunoreactive microglial cells were not affected significantly as indicated by the lack of change in immunoreactive areas ($0.10 \pm 0.012\%$, $0.12 \pm 0.007\%$ and $0.10 \pm 0.014\%$ for mice injected with Ad-VIP, Ad-Blank, and PBS, respectively; Fig. 7A, d-f, 7C). We also investigated CD45-immunoreactive microglial cells to investigate the activation stage of microglia in these transgenic mice.

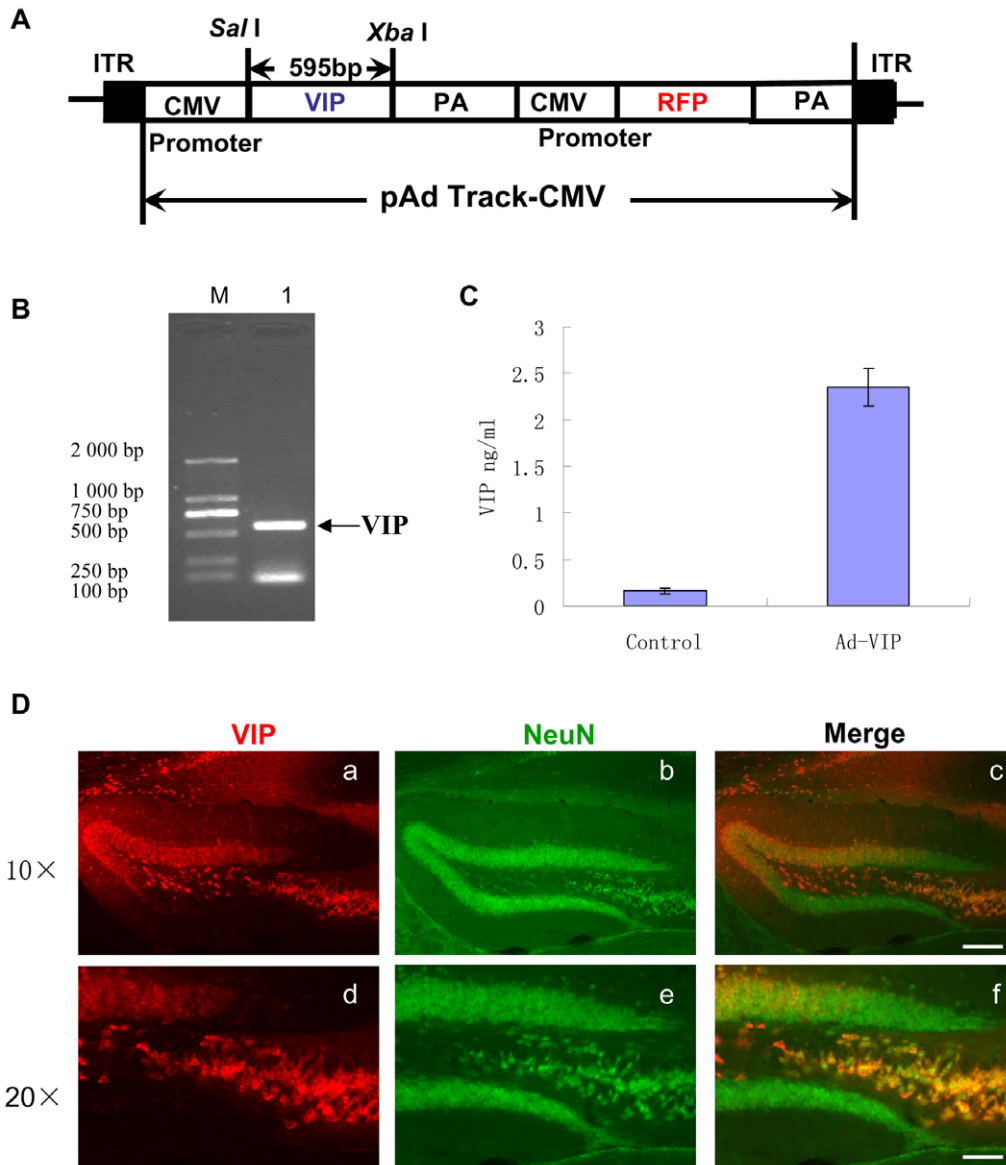


Figure 4. VIP highly expressed in the hippocampus NeuN positive cells after unilateral lateral ventricular injection of Ad-VIP. A: Schematic diagram of VIP adenovirus construction. B: Lane 1 shows the PCR product, corresponding to the mouse VIP cDNA (595 bp). Samples were run on a 2% agarose gel with a DNA ladder (left side). VIP cDNA was also verified by sequencing. C: VIP expression in rAd5CMVhVIP-infected cells. Culture media were assayed for VIP by an ELISA kit. Data shown are the total amount of VIP (ng) per 10^6 infected 293 cells (Multiplicity of infection 320) per 24 h. The results are representative of five experiments with 3 replicates. D: Brain sections were prepared from TgAPPswe/PS1dE9 mice two months after Ad-VIP and subjected to double-immunofluorescence staining of VIP (red) and NeuN (green) using anti-VIP antibody and anti-NeuN antibody. Ad-VIP injected brain showing widespread, high expression of VIP in the hippocampus and somewhat less expression in the neocortex (a, d). NeuN staining showed with green fluorescence protein (b, e) and Merged picture showed (c, f). Scale bars 400 μ m (a through c) and 200 μ m (d through f).

doi:10.1371/journal.pone.0029790.g004

The average CD45 immunoreactive areas in the hippocampus were not significantly different between injection groups ($0.13 \pm 0.013\%$, $0.14 \pm 0.009\%$ and $0.12 \pm 0.012\%$ for mice injected with Ad-VIP, Ad-Blank, and PBS, respectively; Fig. 7A g–i, 7D), consistent with the lack of change in CD11c staining.

Recombinant adenovirus-mediated VIP brain delivery does not increase gliosis and apoptosis in APP/PS1 transgenic mice

High levels of VIP expression activated microglial cells, which may also induce the secretion of neurotoxins (cytokines and NO),

leading to gliosis and apoptosis. To assess the cytotoxic potential associated with recombinant adenovirus-mediated overexpression of VIP, brain sections were subjected to Glial fibrillary acidic protein (GFAP) immunohistochemistry and Terminal (TdT)-mediated dUTP-biotin nick end labeling (TUNEL) assay. The average GFAP immunoreactive area in the hippocampus was $4.41 \pm 0.51\%$ in the Ad-VIP group, $5.8 \pm 0.53\%$ in the Ad-Blank group, and $5.2 \pm 0.58\%$ in the PBS group, indicating that VIP overexpression slightly reduced gliosis compared to Ad-blank treatment, but not significantly ($P = 0.099$, $n = 8$ for each group) (Fig. 8Aa–c). No apoptotic cell death was detected by TUNEL

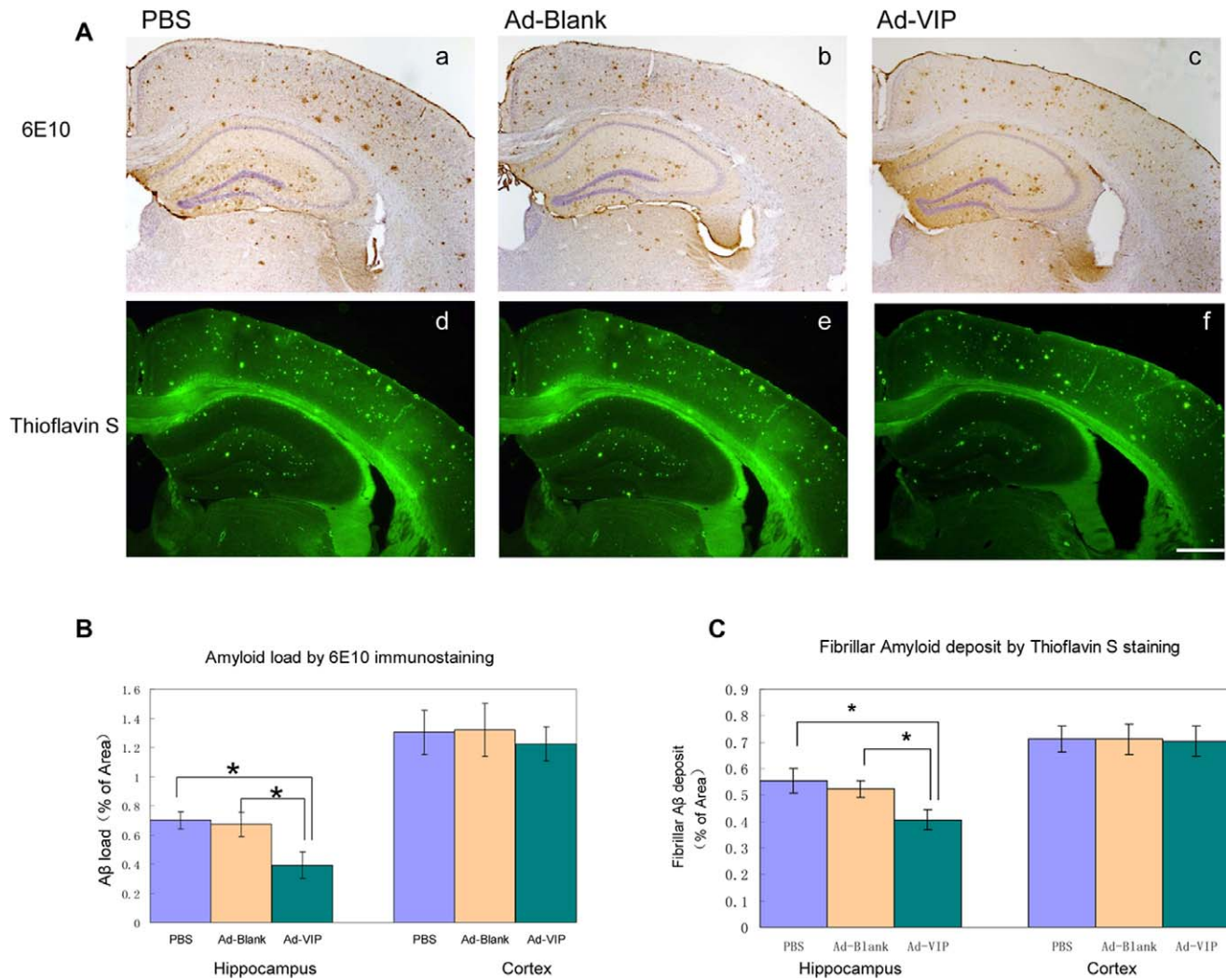


Figure 5. Adenovirus-mediated VIP expression reduces immunoreactive A β deposits and fibrillar A β deposits in the hippocampus but not in the neocortex. (a through h) Two months after Ad-VIP, Ad-Blank, or PBS injection, mice were terminated and A β deposits in the brain were visualized by immunohistochemistry and thioflavine S staining quantified by morphometric analysis. Diffuse and fibrillar A β deposits visualized by 6E10 antibody (a through c) and thioflavine S staining (d through f) in the cerebral cortex and hippocampus from mice injected with PBS (a and d), Ad-Blank (b and e) and Ad-VIP (c and f). The percentages of immunoreactive area for A β and thioflavine S fluorescent, respectively, are shown as bar graphs (g, h). The values shown are the mean \pm S.E.M. Scale bars 400 μ m (a through f). ANOVA and post hoc testing revealed significant differences between different group. * $P < 0.05$. doi:10.1371/journal.pone.0029790.g005

staining in the brains injected with Ad-VIP (Figure 8f), suggesting that adenovirus-mediated VIP overexpression in the hippocampus does not induce neuronal or glial apoptosis.

Discussion

The principal pathological hallmark of Alzheimer's disease is the extracellular deposition of fibrillar A β and its compaction into senile plaques surrounded by activated microglia and astrocytes (reactive gliosis). Microglial activation is a "double-edged" sword in that these cells release proinflammatory cytokines, pro-apoptotic factors and reactive oxygen and nitrogen species in addition to protective neurotrophins. In addition, microglial phagocytosis can protect neurons from toxic substances, such as aggregated A β . Regulating microglial phenotype to enhance protective mechanisms (neurotrophin release and phagocytosis) while suppressing neurotoxic effects could be the basis for novel therapeutic strategies. Consistent with the role of neuropeptides as critical

modulators of the immune response in the CNS [29], we demonstrated that VIP regulated microglial activation by fibrillar-A β_{42} . Indeed, VIP significantly promoted microglia phagocytosis of A β_{1-42} and attenuated cerebral amyloidosis in a transgenic mouse model of AD.

Previous studies examining the effects of VIP on phagocytosis in macrophages yielded conflicting results. Delgado et al concluded that a common denominator in these studies was that VIP stimulated freshly isolated resting macrophages but inhibited prestimulated macrophages. Therefore, the differences in the reported studies could be due to the dominant cell population. In addition, the stimulatory actions of VIP (whether for phagocytosis, adherence and migration, or reactive oxygen production) appear to be associated with PKC activity. Our experiment suggested that the effect of VIP on phagocytosis of microglial cells trend to be stimulatory and associated with PKC activity, Myristoylated protein kinase C peptide inhibitor, which inhibit PKC pathway could efficiently block this effect.

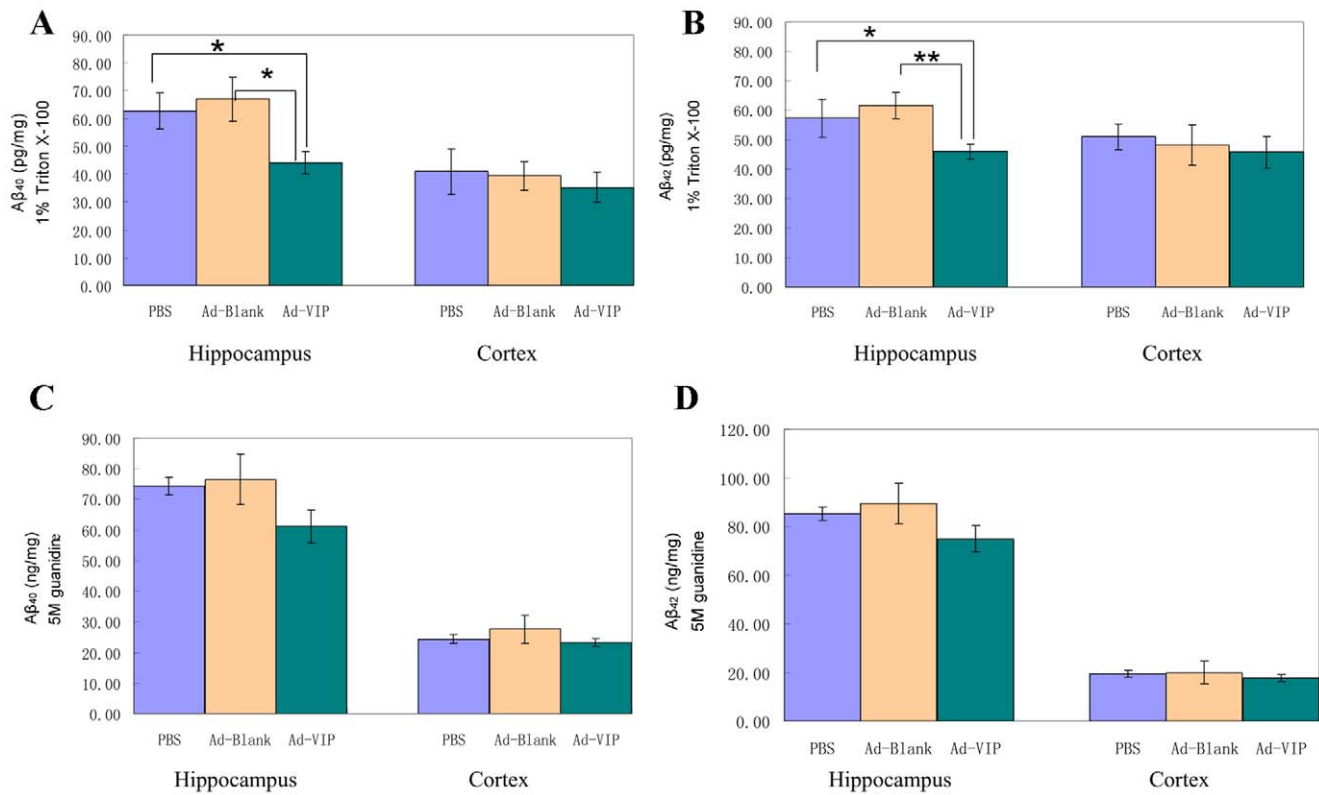


Figure 6. Adenovirus-mediated VIP expression reduces soluble A β_{42} & A β_{40} in the hippocampus at 12 months of age. A, B: The buffer-soluble A β_{42} & A β_{40} contents in different treated Tg mice were quantified by ELISA. The results are shown as bar graphs (means \pm SEM pg/mg protein). * P <0.05. C, D: The buffer-insoluble A β_{42} contents in different treated Tg mice were quantified by ELISA. The results are shown as bar graphs (means \pm SEM ng/mg protein).

doi:10.1371/journal.pone.0029790.g006

Injection of Ad-VIP into the lateral ventricle of PS1/APP transgenic mouse induced significant VIP overexpression and attenuated immunoreactive A β deposits and fibrillar A β deposits in the hippocampus two months after injection. In contrast, A β levels in the cortex were not altered. These restricted effects of VIP may be due to the limited expression of VIP outside the hippocampus. To study the cellular mechanism of A β clearance, we measured changes in microglial and astrocytic immunoreactivity. Surprisingly, we found that CD11b-immunoreactive microglial cells accumulated in the Ad-VIP-injected PS1/APP transgenic mouse hippocampus relative to Ad-blank- or PBS-injected PS1/APP transgenic mice, while CD11c-immunoreactive microglial cells were not significantly altered by Ad-VIP-mediated VIP overexpression. The activation of CD11b-positive microglial cells may be due to VIP-induced activation of cAMP and PI-3K signaling pathways [30]. A previous study demonstrated that CD11b-positive microglial cells trend to have enhanced phagocytotic activity while CD11c-positive microglial cells trend to initiate antigen presentation in response to cytokine secretion [6]. Recently, Nada Choucair-Jaafar reported that an antibody against CD11b reduced the uptake of artificial amyloid deposits by microglia, further indicating that CD11b+ microglia are involved in A β clearance [31]. These results may also partially explain why the A β load was reduced in the hippocampus of AD-VIP-treated mice. In contrast, adenovirus-mediated VIP brain delivery did not increase GFAP expression by astrocytes or neurocellular TUNEL staining, indicating that VIP overexpression did not induce astrogliosis or apoptosis in APP/PS1 transgenic mice. Thus, recombinant adenovirus Ad-VIP injections may be a feasible and

safe treatment to promote the protective effects of microglial cells without deleterious side effects.

In addition to promoting A β accumulation, VIP also blocked A β -induced microglial TNF- α and NO secretion, consistent with previous studies [24]. As a central inflammatory mediator, TNF- α plays a key role in neuronal death mediated by activated microglia. Elevated TNF- α levels were detected in the serum and CSF of AD patients, as well as in cortical and glial cell cultures after exposure to A β . Furthermore, high levels of TNF- α induced apoptosis of cortical neurons by activating the neuronal TNF- α receptor [32,33]. Activated microglia also release NO, which can form highly neurotoxic NO $_2^-$. Weldon et al. demonstrated that NO secreted by activated microglia could kill culture human fetal neurons by apoptosis [34]. Many immune activators, such as LPS, can promote microglial phagocytosis of A β and reduce the A β load in transgenic mice [35]. However, most of these agents can not inhibit concomitant microglial TNF- α or NO secretion, and may even increase TNF- α and NO secretion, which abate the possible clinical application. Recently, Delgado et al showed that VIP efficiently inhibited the secretion of cytokines associated with microglial activation induced by A β [24]. Consider with Our study that the presence of VIP resulted in a significant promotion of microglial phagocytosis of fibrillized-A β , hinting that VIP may be an ideal treatment for AD.

Studies addressing the neuroprotective efficacy of VIP in a Parkinson's disease model revealed that VIP could prevent MPTP-induced nigrostriatal dopaminergic neuronal death by blocking microglial activation [36]. Furthermore, Gozes et al found that the A β -induced cortical neuronal death was completely prevented by

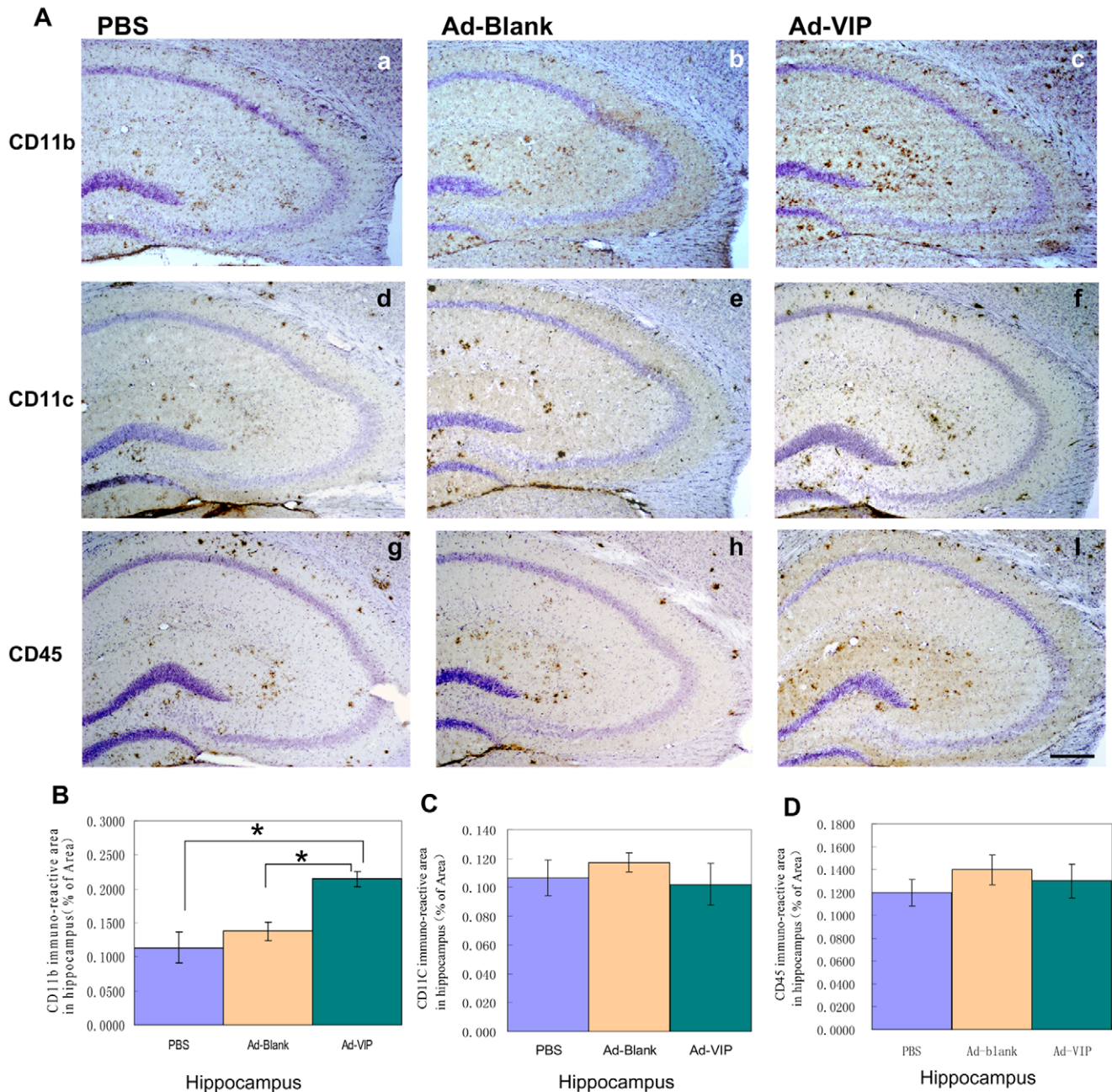


Figure 7. CD11b but not CD11c or CD45 immunoreactive microglia significantly activated in the hippocampus of Ad-VIP injected mice. A: (a–f) Brain sections from mice injected with PBS (a), Ad-Blank (b) and Ad-VIP (c) were stained with anti-CD11b antibody or anti-CD11c(d,e,f) antibody or anti-CD45(g,h,i) antibody. Scale bars are 200 μ m in a through i. B: CD11b immunoreactive quantified by morphometric analysis. CD11b immunoreactive area percentages in the hippocampus are shown as a bar graph (means \pm S.E.M.) * P <0.05. C: CD11c immunoreactive quantified by morphometric analysis. CD11c immunoreactive area percentages in the hippocampus are shown as a bar graph (means \pm S.E.M.). D: CD45 immunoreactive quantified by morphometric analysis. CD1145 immunoreactive area percentages in the hippocampus are shown as a bar graph (means \pm S.E.M.).
doi:10.1371/journal.pone.0029790.g007

co-treatment with 0.1 pM [St-Nle7] VIP and that St-Nle-VIP injected intracerebroventricularly or delivered intranasally prevented impairments in spatial learning and memory associated with cholinergic blockade in a rat cholinergic deficits model [37]. Neuroinflammation may be a pathogenic mechanism common to several neurodegenerative diseases, so VIP may be widely applicable as a neuroprotective agent by suppressing the pathological activities of activated microglia.

In summary, our results demonstrated that VIP promoted microglia phagocytosis of A β and suppressed the A β -induced release of microglial neurotoxins. Furthermore, constitutive overexpression of VIP in the hippocampus reduced inflammation and attenuated amyloidosis in a transgenic mouse model of AD. Modulation of A β -induced microglia activation and microglial phenotype by delivery of VIP into the brain may be a novel approach for the treatment of Alzheimer's diseases.

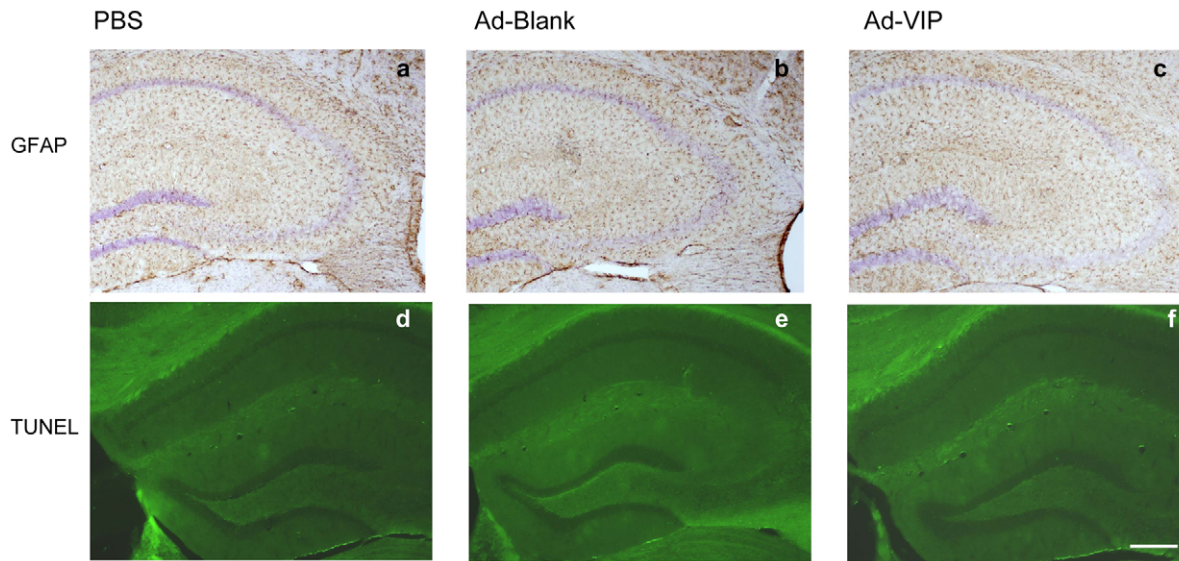


Figure 8. Recombinant adenovirus-mediated VIP brain delivery does not increase gliosis and apoptosis. (a–f) Brain sections from mice injected with PBS (a), Ad-Blank (b) and Ad-VIP (c) were stained with anti-GFAP antibody and Apoptotic cells identified by TUNEL staining (d, e, f). Scale bars are 200 μ m in a through f.

doi:10.1371/journal.pone.0029790.g008

Materials and Methods

Reagents

β -Amyloid peptide(A β)1–42, Cy3 conjugated A β 1–42 peptides were purchased from Biosource International (Camarillo, CA). The peptides were pre-aggregated for 24 h at 37°C in complete medium. Vasoactive Intestinal Peptide was obtained from Sigma (St. Louis, MO) and dissolved in 0.01 M phosphate-buffered saline (PBS) to a stock concentration of 10⁻⁶ M. Recombined mouse IFN- γ were purchased from BD Pharmingen (San Diego, CA).

Cell Cultures

The murine microglial cell line (N9) was kindly provided by Dr. Ji Ming Wang (Center for Cancer Research, National Cancer Institute, Frederick, USA) and were grown in RPMI 1640 medium supplemented with 5% fetal calf serum, 2 mM glutamine, 100 U/ml penicillin, 0.1 g/ml streptomycin and 0.05 mM 2-mercaptoethanol.

Mouse primary microglial cells culture was prepared as described previously [15]. Briefly, cerebral cortices from newborn C57/BL6 mice (1–2 days old) were isolated under sterile conditions and were kept at 4°C. Cells were mechanically dissociated and plated in 75-cm² flasks, added RPMI 1640 medium supplemented with 5% fetal calf serum, 2 mM glutamine, 100 U/ml penicillin, 0.1 μ g/ml streptomycin, and 0.05 mM 2-mercaptoethanol. Primary cultures were kept for 14 days so that only glial cells remained and microglial cells were isolated by shaking flasks at 200 rpm in a Lab-Line incubator-shaker. More than 98% of these glial cells stained positively for CD11b (BD Pharmingen, San Diego, CA). All animals were provided by animal center of Third Military Medical University and all experiments were in compliance with protocols (IACUC: 06512) approved by the Third Military Medical University Institutional Animal Care and Use Committee.

Microglia A β phagocytosis assays

Primary mouse microglia were seeded at 1 \times 10⁵ cells/well (n = 6 for each condition) in 24-well tissue culture plates containing

0.5 mL of complete RPMI 1640 medium. These cells were treated for 2 h with “aged” A β _{1–42} conjugated with Cy3 (Biosource International; 500 nM pre-aggregated for 24 h at 37°C in complete medium). In the presence of Cy3-A β _{1–42}, microglial cells were then treated with VIP, LPS. Some of these cells were treated with PMA (30 nM), Forskolin (10 μ M), Myristoylated protein kinase C peptide (50 μ M) combined with VIP, PKA inhibitor fragment 14–22 myristoylated trifluoroacetate salt (PKA Inhibitor) (5 μ M) (Sigma, St. Louis, MO) combined with VIP in the presence of Cy3-A β _{1–42} for 2 h. Microglial cells were then rinsed three times in complete medium, and the media were exchanged with fresh complete medium for 10 minutes to allow for removal of non-incorporated A β _{1–42} and promote concentration of A β _{1–42} into phagosomes. Extracellular and cell-associated Cy3-A β _{1–42} were quantified using an MSF (SpectraMaxH, Molecular Devices) with an emission wavelength of 590 nm and an excitation wavelength of 543 nm.

A standard curve from 0 to 600 nM of Cy3-A β was run for each plate. Total cellular proteins were quantified using the Micro BCA Protein Assay (Pierce, Rockford, IL). The mean fluorescence values for each sample at 37°C and 4°C at the 2 h point were determined by fluorometric analysis. Relative fold change values were calculated as: mean fluorescence value for each sample at 37°C / mean fluorescence value for each sample at 4°C. In this manner, both extracellular and cell-associated Cy3-A β _{1–42} were quantified. Considering nonspecific adherence of A β to the plastic surface of culture plates, an additional control without cells was carried out through all of experiments above. An incubation time of less than 4 h did not change the amount of A β _{1–42} peptide detected in the supernatant. In order to determine the extent to which cell death might have influenced the phagocytic activity in the various treatment groups, we performed the LDH assay on the relevant supernatant. Data showed that there was no significant cell death occurring over the 3 h time frame in any of the treatment groups.

Fluorescence microscope examination

Microglial cells (wild-type primary cultured microglial cells or N9) phagocytosis of fibrillar A β _{1–42} peptides was carried out

similarly to previously described protocols [38], Microglial cells were cultured at 2×10^5 /well in 12-well tissue-culture plates with glass inserts for fluorescence microscopy. On the following day, microglia cells were treated with Cy3-conjugated A β _{1–42} (500 nM) in the presence or absence of VIP (10^{-8} M) for a different phase of time. As a positive control, microglial cells were treated with Cy3-conjugated A β _{1–42} (500 nM) combined with LPS(100 ng/mL, Sigma). In parallel dishes, microglial cells were incubated with Cy3-conjugated A β _{1–42} under the same treatment conditions as described above, except that they were incubated at 4°C to control for nonspecifically cellular association of Cy3-A β _{1–42}. Microglial cells were then rinsed 3 times in Cy3-A β _{1–42}-free complete medium and the media was exchanged with fresh Cy3-A β _{1–42}-free complete medium for 10 min both to allow for removal of non-incorporated Cy3-A β _{1–42} and to promote concentration of the Cy3-A β _{1–42} peptide into phagosomes. This medium was withdrawn, and microglia were rinsed 3 times with ice-cold PBS. For fluorescence microscope examination, these Microglial cells will be washed 5 times with ice-cold PBS to remove extracellular A β and fixed in 4% paraformaldehyde(PFA) diluted in PBS. After three successive rinses in TBS, microglia nuclei were detected by incubation with DAPI for 10 min and finally mounted with fluorescence mounting media containing Slow Fade antifading reagent (Molecular Probes, Eugene, OR), and then viewed under a BX61 microscope (Olympus, Tokyo, Japan) equipped with a digital camera. The data was digitized using an attached Image Pro Plus imaging system (MediaCybernetics).

Cytokine analysis

Microglial cells (N9 or wild-type primary cultured microglial cells) were plated in 24-well tissue-culture plates (Costar, Cambridge, MA) at 1×10^5 cells per well and stimulated for 24 hr with either A β _{1–42} (2.5 μ M) or a dose range of IFN- γ (10 U/mL, 200 U/mL)/A β _{1–42} (2.5 μ M) in the presence or absence of VIP (10^{-8} M). Cell-free supernatants were collected and stored at -70°C until analysis. TNF- α cytokine and NO levels in the supernatants were examined using specific enzyme-linked immunosorbent assay (ELISA) kits (R&D Systems) or Griess Reagent Kit for Nitrite Determination (Promega) in strict accordance to the manufacturer's protocols. The results of TNF- α cytokine are shown as mean picograms of each cytokine per milliliter (\pm SD) and The results of NO represent as mean μM (\pm SD).

Recombinant adenovirus preparation

Recombinant adenovirus pAdeasy-VIP (1×10^{11} PFU/ml) and blank adenovirus(1×10^{11} PFU/ml) was generated by Min Song according to the methods [28] (Department of medical genetics, Third Military Medical University), Briefly, VIP was amplified by RT-PCR and cloned into a shuttle pAd Track-CMV vector with Red fluorescence Protein (RFP) tag. This plasmid was linearized by digesting with restriction endonuclease PmeI and subsequently cotransformed into Escherichia coli BJ5183 cells with an adenoviral backbone pAdEasy-1 plasmid. Recombinants were selected by kanamycin resistance. Finally, recombinants were transfected into HEK293 cells. Recombinant adenoviruses were generated within 7–10 d. then purified with Sartbind Q5 column purification system(Sartorius stedim biotech, Aubagne Cedex, France). The titers of Adenovirus were determined by the quantitative fluorescence assay as described previously [39]. A control null Adenovirus (Ad-blank) which only express Red fluorescence Protein was similarly prepared. VIP protein expression was determined by ELISA kit (Peninsula Laboratories, San Carlos, CA, USA), Typically, 2×10^2 particles of Ad-VIP vector/cell

resulted in almostly 20-fold increase over background in the culture medium per 10^6 infected 293 cells.

Experimental animals and stereotaxic injection of Ad-VIP

Tg(APP^{swe}, PSEN1^{de9}) mice (line B6C3-85Dbo/J) were purchased from Jackson Laboratory (Bar Harbor, ME). The transgenic mice express chimeric mouse/human APP with the double mutations (K670N and M671L) and human PS1 with a deletion of exon 9 found in familial AD patients. Animals were housed and maintained at the College of Medicine Animal Facility of the Third Military Medical University. A total of forty-five 10 months old Tg PS1/APP^{sw} mice were randomly assigned to 3 treatment groups in such a manner as there was no significant intergroup difference in body weight: PBS, Ad-blank, Ad-VIP (n = 15 for each group, 8 mice for histochemical analyses and 7 mice for protein analysis).

The intra-lateral ventricle injections surgery procedure was according with Giovanni DiCarlo described previously [35]. Briefly, the mice were weighed, anesthetized with pentobarbital and placed in a stereotaxic apparatus (51603 dual manipulator lab standard, Stoelting, Wood Dale, IL). A midsagittal incision was made to expose the cranium, A hole in the skull was made by a drill 0.5 mm posterior to the bregma and 1.0 mm right to the midline. A 10 μ l injection of PBS or recombinant adenovirus Ad-VIP (1×10^{11} PFU/ml) or blank adenovirus, Ad-blank(1×10^{11} PFU/ml) was made using a 10 μ l syringe (Hamilton, Reno, Nevada) was injected unilaterally into the right ventricle at the depth of 2 mm at a rate of 1 μ l/min. After allowing the needle to remain in place for 5 min, the needle was slowly raised at a rate of 0.1 cm/min. Two months after the injection, the experimental animals were terminated to determine the therapeutic effects of the treatment. All animal protocols (IACUC: 06513) used for this study were prospectively reviewed and approved by the Institutional Animal Care and Use Committee of Third Military Medical University Institutional Animal Care and Use Committee.

Immunohistochemical and histochemical analyses

Mice were deeply anesthetized with pentobarbital and cardinally perfused with cold PBS followed by 4% paraformaldehyde. The brain was quickly removed and fixed in 4% paraformaldehyde for 16 h.

The brains were then stored overnight in 30% sucrose in 0.1 M PBS and frozen in Tissue-Teck optimal cutting temperature compound. coronal sections (35 μ m thick) of the brains were cut on a freezing-stage cryotome and kept in 0.1 M PBS at 4°C. Sections were subjected to immunohistochemical, histochemical, and TUNEL staining. For immunohistochemistry, free floating immunohistochemistry was performed using avidin-biotin immunoperoxidase method (Vector, Burlingame, CA). Endogenous peroxidase was eliminated by treatment with 1% H₂O₂/10% methanol Tris-buffered saline (TBS) for 60 min at room temperature. After washing with 0.1 M Tris buffer (pH 7.5) and 0.1 M TBS (pH 7.4), sections were blocked with 5% normal serum (from the same animal species in which the secondary antibody was made) in 0.1 M TBS with 0.5% triton-X-100 (TBS-T) for 60 min at room temperature to prevent non specific protein binding. The sections were then incubated with primary antibodies as described above and 6E10 for detection of A β in 2% serum in TBS-T for 18–48 h at 4°C. The sections were rinsed in 0.1 M TBS and incubated with biotinylated secondary antibodies in 2% serum TBS-T for 2 h at room temperature. Finally, the avidin biotin peroxidase method using 3, 3'-diaminobenzidine as a substrate (Vector, Burlingame, CA) was performed according to manufacturer's protocol. For the negative

control, slides were processed without primary antibody. Some sections were counterstained with hematoxylin. For thioflavine S staining, tissue sections were stained in 1% thioflavine S (Sigma) and rinsed with 70% ethanol. After washing with H₂O, the sections were mounted in 75% glycerol in H₂O. Neuroinflammation was detected by staining the brain sections with rat anti-mouse CD11b, rat anti-mouse CD11c, rat anti-mouse CD45, rabbit anti-mouse GFAP antibodies BD Pharmingen (San Diego, CA).

Immunofluorescence

Free-floating brain sections were used to analyze Adenovirus mediated VIP expression, Immunofluorescence detection and staining for VIP and NeuN was performed using the anti-NeuN antibody (1:400). Sections were incubated in anti-NeuN antibodies overnight at 4°C, rinsed in PBS, and incubated for 1 h in fluorescently labeled secondary antibodies. Sections were washed three times with PBS. To assess nonspecific labeling, a negative control sample was processed using the same protocol but with the primary antibody omitted. Cells were counted with a BX61 microscope (Olympus, Tokyo, Japan) equipped with a digital camera.

Quantification of buffer soluble and in-soluble brain A β by ELISA

The treated Mice ($n = 7$ for each group) were deeply anesthetized with pentobarbital and cardinally perfused with cold PBS. The isolated hippocampus and cortex were weighted and then placed in ice-cold lysis buffer, sonicated on ice for ~ 3 min, allowed to stand for 15 min at 4°C, and centrifuged at 15,000 rpm for 15 min. Levels of buffer-soluble and insoluble A β in the hippocampus were determined by the A β ₄₂ and A β ₄₀ ELISA kits (Invitrogen, Carlsbad, CA) according to the manufacturer's protocol. Levels of buffer-soluble A β were expressed as mean pg/mg of total protein in tissue lysate standard error. Levels of buffer-insoluble A β were expressed as mean ng/mg of wet tissue weight standard error.

TUNEL assay to detect apoptosis

To investigate cytotoxicity possibly associated with the therapeutic modalities, brain sections were subjected to Terminal (Td)T-mediated dUTP-biotin nick end labeling (TUNEL) assay using the In situ Cell Death Detection Kit (Roche Biochemicals, Indianapolis, IN) according to the manufacturer's protocol. Slides were analyzed using a BX61 microscope (Olympus, Tokyo, Japan) equipped with a digital camera.

References

- Hardy J, Selkoe DJ (2002) The amyloid hypothesis of Alzheimer's disease: progress and problems on the road to therapeutics. *Science* 297: 353–356.
- Henry W, Querfurth FL (2010) Alzheimer's disease. *N Engl J Med* 362: 329–44.
- Wyss-Coray T (2006) Inflammation in Alzheimer disease: driving force, bystander or beneficial response? *Nat Med* 12: 1005–1015.
- Rivest S (2009) Regulation of innate immune responses in the brain. *Nat Rev Immunol* 9: 429–439.
- Mandrekar-Colucci S, Landreth GE (2010) Microglia and inflammation in Alzheimer's disease. *CNS Neurol Disord Drug Targets* 9: 156–167.
- Monsonogo A, Weiner HL (2003) Immunotherapeutic approaches to Alzheimer's disease. *Science* 302: 834–8.
- Reinke E, Fabry Z (2006) Breaking or making immunological privilege in the central nervous system: the regulation of immunity by neuropeptides. *Immunol Lett* 104: 102–9.
- Liu J, Chen M, Wang X (2000) Calcitonin gene-related peptide inhibits lipopolysaccharide-induced interleukin-12 release from mouse peritoneal macrophages, mediated by the cAMP pathway. *Immunology* 101: 61–7.
- Wu R, Zhou M, Wang P (2003) Adrenomedullin and adrenomedullin binding protein-1 downregulate TNF-alpha in macrophage cell line and rat Kupffer cells. *Regul Pept* 112: 19–26.
- Bedoui S, Miyake S, Lin Y, Miyamoto K, Oki S, et al. (2003) Neuropeptide Y (NPY) suppresses experimental autoimmune encephalomyelitis: NPY1 receptor-specific inhibition of autoreactive Th1 responses in vivo. *J Immunol* 171: 3451–8.
- Muhvic D, Radosvic-Stasic B, Pugal E, Rukavina D, Sepcic J, et al. (1992) Modulation of experimental allergic encephalomyelitis by somatostatin. *Ann N Y Acad Sci* 650: 170–8.
- Delgado M, Pozo D, Ganea D (2004) The significance of vasoactive intestinal peptide in immunomodulation. *Pharmacol Rev* 56: 249–90.
- Gonzalez-Rey E, Delgado M (2005) Role of vasoactive intestinal peptide in inflammation and autoimmunity. *Curr Opin Investig Drugs* 6: 1116–23.
- Loren I, Emson PC, Fahrenkrug J, Bjorklund A, Aluets J, et al. (1979) Distribution of vasoactive intestinal polypeptide in the rat and mouse brain. *Neuroscience* 4: 1953–76.

Image analysis

Quantitative image analysis was performed for amyloid deposits and reactive/activated glial cells immunohistochemistry in Tg PS1/APPsw mice injected with Recombinant adenovirus Ad-VIP or blank adenovirus or PBS. Images were performed using an Olympus BX61 automated microscope, Olympus Fluoview system and the Image Pro Plus v5 image analysis software (Media Cybernetics, Silver Spring, MD). Briefly, images of five 35 μ m sections each separated by an approximately 400 μ m interval, starting at 1.3 mm posterior to the bregma to caudal, from each mouse were analyzed. Both neocortex and hippocampus were found in all the brain sections and analyzed separately. Stained areas were expressed as a percentage of total neocortex or hippocampus, respectively. A threshold optical density was obtained that discriminated staining from background. Manual editing of each field was used to eliminate artifacts. Data are reported as a percentage of immuno-labeled area captured (positive pixels) divided by the full area captured (total pixels). Quantitative image analysis was performed by a single examiner (T.M.) blinded to sample identities. Data were expressed as mean \pm standard error of the mean (SEM) as a bar graph.

Statistical analysis

All data were normally distributed; therefore, in instances of single mean comparisons, Levene's test for equality of variances followed by a *t* test for independent samples was used to assess significance. In instances of multiple mean comparisons, ANOVA was used, followed by post hoc comparison using Bonferroni's method. α Levels were set at 0.05 for all analyses. The statistical package for the social sciences release 10.0.5 (SPSS, Chicago, IL) was used for all data analyses.

Acknowledgments

The authors thank Prof. Bing Ni for support (Immunology institute of Third Military Medical University, Chongqing, China) on animal experiment and Wei Sun (Central Laboratory of Third Military Medical University, Chongqing, China) for technical support.

Author Contributions

Conceived and designed the experiments: YB MS. Performed the experiments: MS JXX YYW JT. Analyzed the data: MS JXX YYW JT BZ. Wrote the paper: MS.

15. Farmery SM, Owen F, Poulter M, Crow TJ (1984) Characterisation and distribution of vasoactive intestinal polypeptide binding sites in human brain. *Neuropharmacology* 23: 101–4.
16. Joo KM, Chung YH, Kim MK, Nam RH, Lee BL, et al. (2004) Distribution of vasoactive intestinal peptide and pituitary adenylate cyclase-activating polypeptide receptors (VPAC1, VPAC2, and PAC1 receptor) in the rat brain. *J Comp Neurol* 476: 388–413.
17. Delgado M, Jonakait GM, Ganea D (2002) Vasoactive intestinal peptide and pituitary adenylate cyclase-activating polypeptide inhibit chemokine production in activated microglia. *Glia* 39: 148–61.
18. Martinez C, Abad C, Delgado M, Arranz A, Juarranz MG, et al. (2002) Anti-inflammatory role in septic shock of pituitary adenylate cyclase-activating polypeptide receptor. *Proc Natl Acad Sci U S A* 99: 1053–8.
19. Grimm MC, Newman R, Hassim Z, Cuan N, Connor SJ, et al. (2003) Cutting edge: vasoactive intestinal peptide acts as a potent suppressor of inflammation in vivo by trans-deactivating chemokine receptors. *J Immunol* 171: 4990–4.
20. Glowa JR, Panlilio LV, Brenneman DE, Gozes I, Fridkin M, et al. (1992) Learning impairment following intracerebral administration of the HIV envelope protein gp120 or a VIP antagonist. *Brain Res* 570: 49–53.
21. Gozes I, Glowa J, Brenneman DE, McCune SK, Lee E, et al. (1993) Learning and sexual deficiencies in transgenic mice carrying a chimeric vasoactive intestinal peptide gene. *J Mol Neurosci* 4: 185–193.
22. Arai H, Moroji T, Kosaka K (1984) Somatostatin and vasoactive intestinal polypeptide in postmortem brains from patients with Alzheimer-type dementia. *Neurosci Lett* 52: 73–8.
23. Zhou JN, Hofman MA, Swaab DF (1995) VIP neurons in the human SCN in relation to sex, age, and Alzheimer's disease. *Neurobiol Aging* 16: 571–6.
24. Delgado M, Varela N, Gonzalez-Rey E (2008) Vasoactive intestinal peptide protects against beta-amyloid-induced neurodegeneration by inhibiting microglia activation at multiple levels. *Glia* 56: 1091–1103.
25. De la Fuente M, Delgado M, del Rio M, Martinez C, Hernanz A, et al. (1993) Stimulation by vasoactive intestinal peptide (VIP) of phagocytic function in rat macrophages. Protein kinase C involvement. *Regul Pept* 48: 345–53.
26. Tan J, Town T, Paris D, Mori T, Suo Z, et al. (1999) Microglial activation resulting from CD40-CD40L interaction after beta-amyloid stimulation. *Science* 286: 2352–5.
27. Krishnadas A, Onyuskel H, Rubinstein I (2003) Interactions of VIP, secretin and PACAP(1–38) with phospholipids: a biological paradox revisited. *Curr Pharm Des* 9: 1005–12.
28. Lodde BM, Delporte C, Goldsmith CM, Tak PP, Baum BJ (2004) A recombinant adenoviral vector encoding functional vasoactive intestinal peptide. *Biochem Biophys Res Commun* 319: 189–92.
29. Reinke E, Fabry Z (2006) Breaking or making immunological privilege in the central nervous system: the regulation of immunity by neuropeptides. *Immunol Lett* 104: 102–9.
30. El Zein N, Badran B, Sariban E (2008) VIP differentially activates beta2 integrins, CR1, and matrix metalloproteinase-9 in human monocytes through cAMP/PKA, EPAC, and PI-3K signaling pathways via VIP receptor type 1 and FPRL1. *J. Leukoc Biol* 83: 972–981.
31. Choucair-Jaafara N, Laporte V, Levy R, Poindrona P, Lombarda Y, et al. (2011) CD11b can enhance microglia uptake of artificial amyloid deposits. *Fundam Clin Pharmacol* 25: 115–22.
32. Heneka MT, Loschmann PA, Gleichmann M, Weller M, Schulz JB, et al. (1998) Induction of nitric oxide synthase and nitric oxide-mediated apoptosis in neuronal PC12 cells after stimulation with tumor necrosis factor-alpha/lipopolysaccharide. *J Neurochem* 71: 88–94.
33. Combs CK, Karlo JC, Kao SC, Landreth GE (2001) beta-Amyloid stimulation of microglia and monocytes results in TNFalpha-dependent expression of inducible nitric oxide synthase and neuronal apoptosis. *J Neurosci* 21: 1179–88.
34. Weldon DT, Rogers SD, Ghilardi JR, Finke MP, Cleary JP, et al. (1998) Fibrillar beta-amyloid induces microglial phagocytosis, expression of inducible nitric oxide synthase, and loss of a select population of neurons in the rat CNS in vivo. *J Neurosci* 18: 2161–73.
35. DiCarlo G, Wilcock D, Henderson D, Gordon M, Morgan D (2001) Intrahippocampal LPS injections reduce Abeta load in APP+PS1 transgenic mice. *Neurobiol Aging* 22: 1007–12.
36. Delgado M, Ganea D (2003) Neuroprotective effect of vasoactive intestinal peptide (VIP) in a mouse model of Parkinson's disease by blocking microglial activation. *FASEB J* 17: 944–6.
37. Gozes I, Bardea A, Reshef A, Zamostiano R, Zhukovsky S, et al. (1996) Neuroprotective strategy for Alzheimer disease: intranasal administration of a fatty neuropeptide. *Proc Natl Acad Sci U S A* 93: 427–32.
38. Zhu Y, Hou H, Nikolic WV, Ehrhart J, Rrapo E, et al. (2008) CD45RB Is a Novel Molecular Therapeutic Target to Inhibit Ab Peptide-Induced Microglial MAPK Activation. *PLoS ONE* 3(5): e2135.
39. He TC, Zhou Sb, Da Costa LT, Jian Y, Kinzler KW, et al. (1998) A simplified system for generating recombinant adenoviruses. *Proc Natl Acad Sci U S A* 95: 2509–2514.